Summary: We have synthesized a new polyhedral oligomeric silsesquioxane (POSS) containing eight phenol functional groups and copolymerized it with phenol and formaldehyde to form novolac-type phenolic/POSS nanocomposites exhibiting high thermal stabilities and low surface energies. Our DSC results indicate that the glass transition temperature of these nanocomposites increased initially upon increasing their POSS content, but then decreased at POSS content above 10 wt.-%, presumably because of the formation of relatively low molecular weight species and POSS aggregation as evidenced from MALDI-TOF mass analyses. Our TGA analyses indicated that the 5-wt.-%-mass-loss temperatures (T_d) increased significantly upon increasing the POSS content because the incorporation of the POSS led to the formation of an inorganic protection layer on the nanocomposite's surface. XPS and contact angle data provided positive evidence to back up this hypothesis. In addition, contact angle measurements indicated a significant enhancement in surface hydrophobicity after increasing the POSS content.

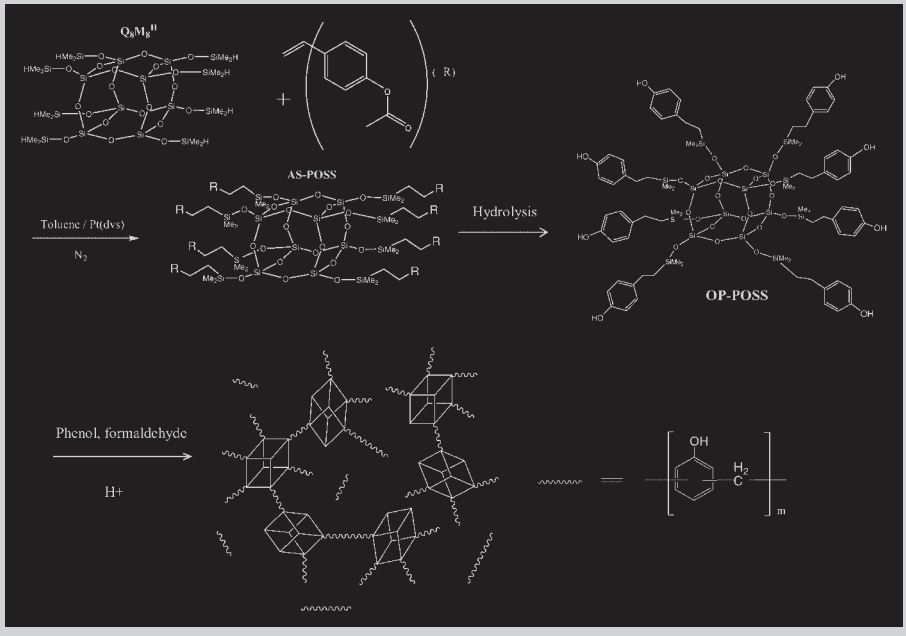

Syntheses procedures of phenolic/OP-POSS nanocomposites.

Thermal and Surface Properties of Phenolic Nanocomposites Containing Octaphenol Polyhedral Oligomeric Silsesquioxane

Han-Ching Lin, Shiao-Wei Kuo, Chih-Feng Huang, Feng-Chih Chang*

Institute of Applied Chemistry, National Chiao Tung University, Hsin Chu, Taiwan
Fax: 886 3 5131512; E-mail: kuosw@mail.nctu.edu.tw

Received: December 15, 2005; Revised: January 27, 2006; Accepted: January 27, 2006; DOI: 10.1002/marc.200500852

Keywords: nanocomposites; phenolic; POSS; resins; surface property

Introduction

Polymers reinforced with well-defined nanosized inorganic clusters (i.e., polymeric nanocomposites) have attracted a tremendous degree of interest because of their potential applications. Among these systems, polyhedral oligomeric silsesquioxanes (POSSs) compounds, which possess unique cage-like structures and nanoscale dimensions, are of particular interest for use as hybrid materials. POSS compounds embody inorganic/organic hybrid architectures, i.e., they contain an inner inorganic framework composed of silicone and oxygen $(SiO_{1.5})_x$ and present organic substituents. Because POSS moieties can be readily incorporated into polymer matrices through copolymerization, many types of polymer/POSS nanocomposites have been synthesized.[1–7]

Phenolic resins are currently irreplaceable materials because they exhibit excellent ablative properties, structural integrity, thermal stability, and solvent resistance. In general, phenolic resins have been practically neglected as materials for use in nanocomposites because they possess three-dimensional structures, even when the resins are not crosslinked, but some effort has been directed toward overcoming this drawback. For example, phenolic-based nanocomposites have been prepared through the sol-gel processing[8] and through intercalative polymerization[9] in the presence of montmorillonite modified with different surfactants. In contrast, very few studies have described the effects that POSSs have on enhancing the properties of phenolic resins,[10] especially their surface properties.

In this study, we developed a simple two-step synthesis of octaphenol-POSS through hydrosilylation of 4-acetoxystyrene with $Q_8M_8^H$ and subsequent hydrolysis of the acetoxy units. This octaphenol-POSS, which possesses eight polymerizable phenol groups, is quite miscible with phenol in solution because of the existence of favorable intermolecular interactions. The eight phenol groups on the periphery of this POSS core copolymerize with phenol and formaldehyde units to form high-molecular-weight novolac-type phenolic/POSS nanocomposites, as illustrated in Scheme 1.

Experimental Part

Syntheses of Phenolic/OP-POSS Nanocomposites

Octa(acetoxystyryl)octasilsesquioxane (AS-POSS) was obtained through the reaction of $Q_8M_8^H$ and 4-acetoxystyrene, as described previously.[11] AS-POSS was dissolved in THF, $NaOH_{(aq)}$ was added, and the hydrolysis was performed at room temperature under nitrogen; it was complete within 2 d. Ethyl ether and deionized water (1:1) were added to the

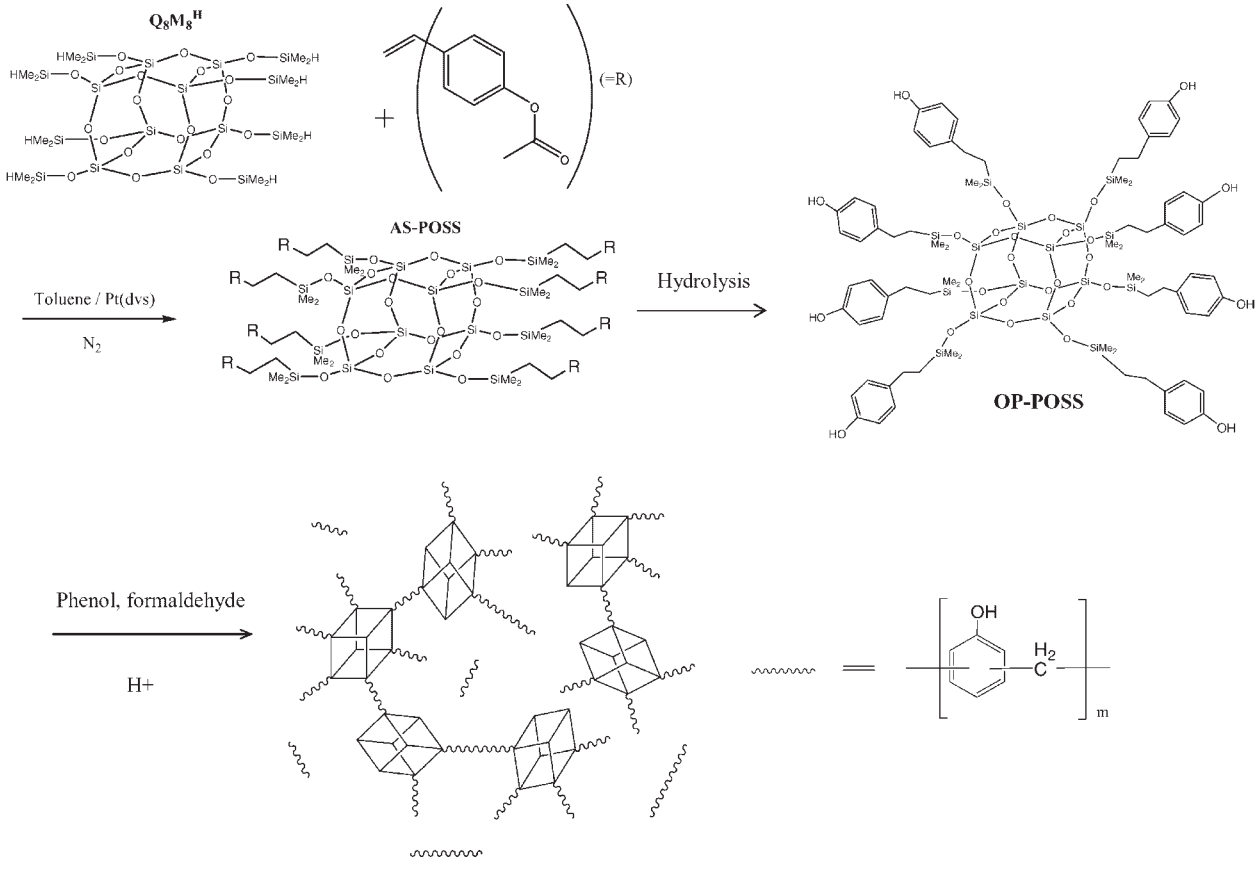

Scheme 1. Synthesis procedure of phenolic/OP-POSS nanocomposites.

Table 1. Formulations and thermal properties of phenolic/OP-POSS nanocomposites.

OP-POSS	OP-POSS	Phenol	Formaldehyde	T_g	T_d	Char yield at 800 °C
wt.-%	g	g	g	°C	°C	wt.-%
0	0	47.44	12.58	82	252	39.8
2	1.23	46.53	12.58	104	311	53.3
5	3.71	45.59	12.58	106	331	53.6
10	6.18	44.65	12.58	96	375	48.2

solution, and then aqueous hydrochloric acid (10 wt.-%) was added slowly with stirring until the pH reached 8. Residual ethyl ether and water were evaporated under vacuum to provide octaphenol-POSS (OP-POSS, $\bar{M}_n = 1\,560$ g·mol^{-1}, PDI = 1.12 by GPC), which was soluble in THF and benzene. The structure of the OP-POSS was confirmed from its ^{1}H NMR and FT-IR spectra.

^{1}H NMR (500 MHz, $CDCl_3$, ppm): $\delta = 6.75–7.13$ (4H, aromatic CH), 4.93 (1H, C_6H_4OH), 2.91 (2H, CCH_2Ar), 1.25 (2H, $SiCH_2C$), 0.54 ppm (6H, $Si(CH_3)_2$).

FT-IR (KBr, cm^{-1}): 3 525 (free OH), 3 350 (hydrogen bonded OH), 3 037 (benzene ring CH stretching), 2 957 (CH_2 stretching), 1 603 (in-plane aromatic C–C stretching), 1 065 (Si–O–Si stretching).

Aqueous formaldehyde and a desired amount of OP-POSS were added into a phenol solution, stirred for 5 min, and then the mixture was added to the flask; Table 1 summarizes the compositions of the phenolic/OP-POSS nanocomposites. Sulfuric acid was added via syringe to the flask and the mixture was then heated at 100 °C under nitrogen; the reaction was completed within 22 h. The solution was washed three times with hot (90 °C) water to remove any unreacted monomer and then it was extracted to remove any residual water. The product was dried in a vacuum oven at 180 °C for 24 h.

Characterization

^{1}H NMR spectra were recorded on a Varian Unity Inova 500 FT NMR spectrometer operated at 500 MHz; deuterated chloroform was used as the solvent. Thermal analyses were performed using a DuPont DSC-9000 differential scanning calorimeter operated at a scan rate of 20 °C·min^{-1} within a temperature range from −50 to 150 °C. Thermal stabilities of the cured samples were investigated using a Du Pont 2050 TGA instrument operated at a rate of 10 °C·min^{-1} from 30 to 800 °C under a nitrogen flow. All mass spectra were recorded using a Bruker Biflex 3 time-of-flight mass spectrometer equipped with a 337-nm nitrogen laser, a 1.25-m flight tube, and a sample target having the capacity to load 384 samples simultaneously; the accelerating potential was set at 19 kV. For contact angle measurements, deionized water and diiodomethane (99%, Aldrich) were chosen as testing liquids because significant amounts of data are available for these liquids. The advancing contact angle measurements of a polymer sample were determined at 25 °C after injecting a liquid drop (5 μL) onto the surface and then using a Krüss GH-100 goniometer interfaced to image-capture software to perform the measurement. We use the two-liquid geometric method to determine the surface energy.[12] For X-ray photoelectron spectroscopy (XPS), samples were spin-coated onto silicon wafers at 1 500 rpm for 45 s; XPS was performed using a VG Microlab 310F spectrometer equipped with an Al K_α X-ray source (1486.6 eV).

Results and Discussion

Figure 1 displays the conventional second-run DSC and TGA thermograms of phenolic/OP-POSS nanocomposites that we prepared at various weight ratios. Each of these hybrids possesses essentially a single value of T_g, suggesting that these hybrids exhibit a single phase. The glass transition temperatures of the nanocomposites were significantly enhanced after incorporation of the POSS units, but suggested that some incompletely reacted functional groups remained on the POSS and phenolic units. We believe that the enhanced glass transition

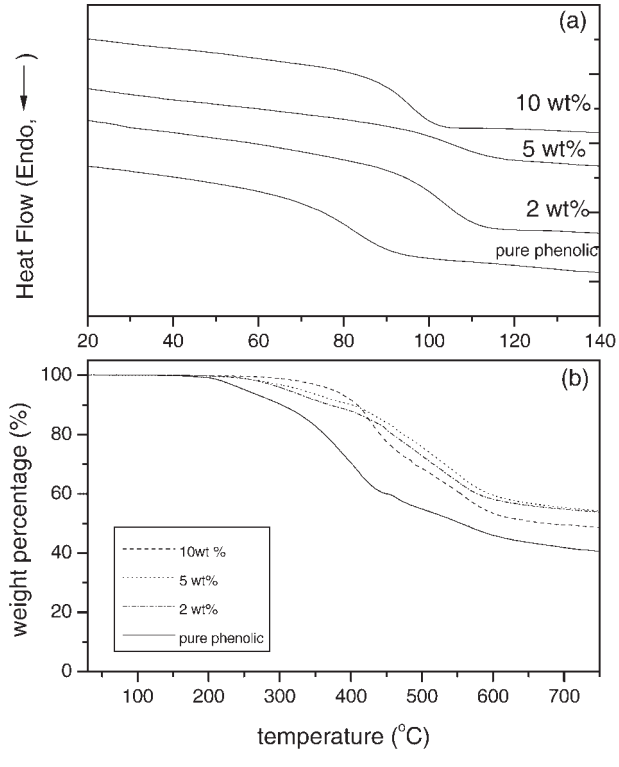

Figure 1. Thermal analyses of phenolic/OP-POSS nanocomposites containing different OP-POSS contents: (a) DSC and (b) TGA.

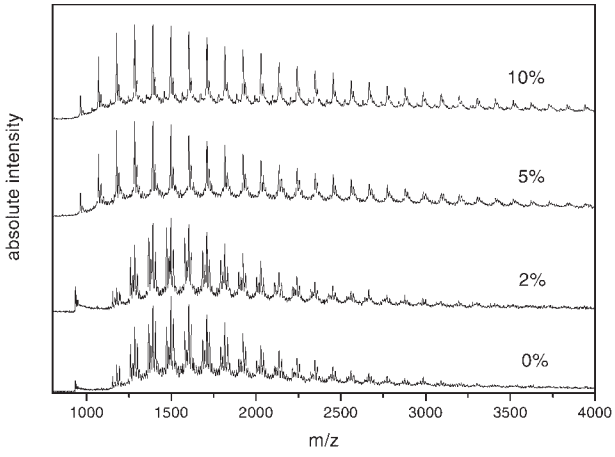

Figure 2. MALDI-TOF mass spectra of phenolic and phenolic/OP-POSS nanocomposites.

temperatures resulted from the restricted motion of the polymer chains that was caused by the even distribution of POSS units on the segmental level.[13] In addition, because phenolic resin contains a high density of hydroxyl groups, strong self-associated hydrogen bonding with the siloxane groups of OP-POSS serves as a physical crosslink that increases the values of T_g of the nanocomposites; we have discussed this phenomenon in depth previously.[14] The values of T_g of these nanocomposites increased upon increasing the POSS content up to 5 wt.-%, but then they decreased unexpectedly at loadings above 10 wt.-%.

To understand this change in behavior of the glass transition temperature of these nanocomposites, we obtained MALDI-TOF mass spectra analyses to monitor the molecular weight distribution. The molar mass distributions of silsesquioxanes can be determined conveniently through the use of UV-MALDI-TOF mass spectrometry.[15] Figure 2 displays the normalized MALDI-TOF mass spectra of the phenolic/OP-POSS nanocomposites that we prepared using various OP-POSS concentrations.

The abundances of low-molecular-weight species ($m/z < 1\,500$) increased upon increasing the POSS content; this finding is consistent with an increasing number of POSS-POSS interactions.[16] In addition, the greater steric hindrance about the aggregated POSS clusters tends to decrease the reactivity of the phenolic groups; this phenomenon results in the production of a relatively larger fractions of low-molecular-weight components and the concomitant decrease in values of T_g. As a result, two competitive factors are involved in determining the final glass transition temperature of the phenolic/OP-POSS nanocomposites: the hindering effects that the POSS cages have on the motion of the polymer chains tends to increase the value of T_g, while the inclusion of the bulky POSS groups tends to increase the free volume of the system and retard the reactivity of the monomers to produce relatively lower MW nanocomposites, i.e., those having lower values of T_g.[17]

We also applied TGA to evaluate the thermal stability of the phenolic/OP-POSS nanocomposites [Figure 1(b)]. Typical of the degradation of phenolic resins, our neat phenolic resin and all of the POSS-containing nanocomposites degraded thermally over three steps. Table 1 summarizes the results of the DSC and TGA analyses, including the 5-wt.-%-mass-loss temperatures (T_d) and the char yields at 800 °C. The char yield increased upon increasing the POSS content, except that it decreased for the sample incorporating 10 wt.-% of POSS, which provides further evidence that lower-molecular-weight species were present in the phenolic/OP-POSS 10 wt.-% sample. The value of T_d increased significantly upon increasing the POSS content; e.g., the phenolic/OP-POSS 10 wt.-% sample exhibited a value of T_d that was 123 °C higher than that of the pure phenolic resin. This phenomenon can be explained in terms of the nanoreinforcement effect of incorporating POSS moieties into polymeric matrixes. The nanoscale dispersion of POSS moieties within the matrix and their covalent and hydrogen bonds to the phenolic resin are responsible for enhancing the initial decomposition temperature. A recent study demonstrated that physical crosslinks formed by POSS units can significantly retard thermal motion; at the same time, they can act as flow aids at elevated

Table 2. Advancing contact angles, surface free energies, and XPS analyses of phenolic/OP-POSS nanocomposites of various compositions.

OP-POSS	Testing liquid		Surface free energy			XPS analysis		
wt.-%	Water	Diiodomethane	γ_s^d	γ_s^p	γ_s	C	O	Si
			$mJ \cdot m^{-2}$	$mJ \cdot m^{-2}$	$mJ \cdot m^{-2}$	%	%	%
0	79.4	42.2	34.5	4.8	39.3	84.9	15.1	0.0
2	91.1	71.0	19.1	4.6	23.7	77.3	11.8	10.9
10	97.0	73.8	18.5	2.8	21.3	67.9	12.1	20.0
After treatment at 210 °C for 24 h								
0	–[a)]	–	–	–	–			
2	77.5	65.0	20.0	10.7	30.7			
10	74.7	66.1	18.8	13.0	31.8			

[a)] The contact angle could not be measured.

temperatures.[18] In addition, the increased values of T_d for the nanocomposites may also result from increased chain spacing, which gives rise to lower thermal conductivity.[19] It was reported recently that the POSS units in related nanostructures prefer to be oriented toward the air-side, an arrangement that screens out the polar groups (e.g., urethane and carboxyl units).[20,21] We anticipated that the POSS moieties in our phenolic/OP-POSS nanocomposites were also oriented toward the air-side to form an inorganic protection layer on the surface of each nanocomposite. To provide evidence in support of this hypothesis, we performed contact angle measurements and XPS analyses to investigate the surface behavior of the nanocomposites. Table 2 lists the surface advancing contact angles and surface energies, measured using two testing liquids (water and diiodomethane), of the pure phenolic resin and of the phenolic/OP-POSS nanocomposites. We used the contact angle data to calculate the polymer surface energy (γ_s), and its polar (γ_s^p) and dispersive (γ_s^d) components, according to the two-liquid geometric method. Strikingly, the phenolic/OP-POSS 10 wt.-% sample had a surface energy (21.3 mJ $\cdot$ m^{-2}) lower than that of poly(tetrafluoroethylene) (PTFE) (22 mJ $\cdot$ m^{-2}, as measured using the same method).[22] Noticeably, the polar component of the surface energy (γ_s^p) was very sensitive to the presence of even a low distribution of POSS moieties; it decreased upon increasing the POSS content.

Table 2 also lists the XPS results, we observed that the atomic percentage of silicon increased dramatically upon increasing the POSS content. Thus, both the contact angle measurements and the XPS results indicate that the POSS moieties were distributed preferably on the surface of the nanocomposite to provide a barrier against the direct contact of the polar phenolic units with the air. To further confirm this structure, we measured the contact angles of samples of pure phenolic resin and phenolic/OP-POSS nanocomposites that we had heated at 210 °C for 24 h; the results are presented in Table 2. After thermal treatment, both testing liquids exhibited complete wetting on the surface of the pure phenolic resin, i.e., we could not measure its contact angles; this phenomenon indicates that the surface properties of the pure phenolic resin changed dramatically after such high-temperature treatment. In contrast, the contact angles of the phenolic/OP-POSS nanocomposites decreased and resulted in higher surface energies, indicating that the incorporation of the POSS moieties enhanced the surface thermal stabilities of these nanocomposites.

Conclusion

We synthesized a series of POSS-based hybrid phenolic resins and characterized their thermal properties and surface free energies. Our DSC and TGA results indicate that the enhancement in the thermal properties was due to strong hydrogen bonding serving as a physical crosslink between the phenolic resin and the OP-POSS units. The results of TGA, XPS, and contact angle analyses all provided evidence that the incorporation of POSS led to the formation of a surface barrier that minimized direct contact of the polar phenolic units with the air. The presence of such a barrier not only enhanced the thermal stability of the bulk and surface of these POSS-containing composites but also led to the surface energy being maintained after treatment at high temperature.

[1] T. S. Haddad, J. D. Lichtenhan, *Macromolecules* **1996**, *29*, 7302.
[2] M. J. Abad, L. Barral, D. P. Fasce, R. J. J. Williams, *Macromolecules* **2003**, *36*, 3128.
[3] Y. Liu, F. Meng, S. Zheng, *Macromol. Rapid Commun.* **2005**, *26*, 926.
[4] H. Li, S. Zheng, *Macromol. Rapid Commun.* **2005**, *26*, 196.
[5] C. M. Leu, Y. T. Chang, K. H. Wei, *Macromolecules* **2003**, *36*, 9122.
[6] Q. Chen, R. Xu, J. Zheng, D. Yu, *Macromol. Rapid Commun.* **2005**, *26*, 1878.
[7] B. X. Fu, W. Zhang, B. S. Hsiao, G. Johansson, B. B. Sauer, S. Phillips, R. Balnski, M. Rafailovich, J. Sokolov, *Polym. Prepr.* **2000**, *41*, 587.
[8] C. C. M. Ma, S. C. Sung, F. Y. Wang, L. Y. Chiang, L. Y. Wang, C. L. Chiang, *J. Polym. Sci., Polym. Phys.* **2001**, *39*, 2436.
[9] H. Y. Byun, M. H. Choi, J. Chung, *Chem. Mater.* **2001**, *13*, 4221.
[10] C. U. Pittman, Jr., G.-Z. Li, H. Ni, *Macromol. Symp.* **2003**, *196*, 301.
[11] S. W. Kuo, H. C. Lin, W. J. Huang, C. F. Huang, F. C. Chang, *J. Polym. Sci., Polym. Phys.* **2006**, *44*, 673.
[12] F. W. Fowkes, "*Adhesion and Adsorption of Polymers, Polymer Science and Technology*", L. H. Lee, Ed., Plenum Press, New York 1980, Vol. 12A, p. 43.
[13] M. Goldman, L. Shen, *Phys. Rev.* **1966**, *114*, 321.
[14] Y. J. Lee, S. W. Kuo, W. J. Huang, H. Y. Lee, F. C. Chang, *J. Polym. Sci., Polym. Phys.* **2004**, *42*, 1127.
[15] W. E. Wallace, C. M. Guttman, J. M. Antonucci, *J. Am. Soc. Mass Spectrom.* **1999**, *10*, 224.
[16] H. Xu, S. W. Kuo, C. S. Lee, F. C. Chang, *Macromolecules* **2002**, *35*, 8788.
[17] Y. Ni, S. Zheng, *Chem. Mater.* **2004**, *16*, 5141.
[18] S. H. Phillips, T. S. Haddad, S. J. Tomczak, *Curr. Opin. Solid State Mater. Sci.* **2004**, *8*, 21.
[19] H. Liu, S. Zheng, K. Nie, *Macromolecules* **2005**, *38*, 5088.
[20] S. Turri, M. Levi, *Macromolecules* **2005**, *38*, 5569.
[21] S. Turri, M. Levi, *Macromol. Rapid Commun.* **2005**, *26*, 1233.
[22] U. Yoshimasa, N. Takashi, *Langmuir* **2005**, *21*, 2614.